

Nanofabricated tips for device-based scanning tunneling microscopy

Leeuwenhoek, Maarten; Norte, Richard A.; Bastiaans, Koen M.; Cho, Doohee; Battisti, Irene; Blanter, Yaroslav M.; Gröblacher, Simon; Allan, Milan P.

DOI

[10.1088/1361-6528/ab1c7f](https://doi.org/10.1088/1361-6528/ab1c7f)

Publication date

2019

Document Version

Final published version

Published in

Nanotechnology

Citation (APA)

Leeuwenhoek, M., Norte, R. A., Bastiaans, K. M., Cho, D., Battisti, I., Blanter, Y. M., Gröblacher, S., & Allan, M. P. (2019). Nanofabricated tips for device-based scanning tunneling microscopy. *Nanotechnology*, *30*(33), [335702]. <https://doi.org/10.1088/1361-6528/ab1c7f>

Important note

To cite this publication, please use the final published version (if applicable).
Please check the document version above.

Copyright

Other than for strictly personal use, it is not permitted to download, forward or distribute the text or part of it, without the consent of the author(s) and/or copyright holder(s), unless the work is under an open content license such as Creative Commons.

Takedown policy

Please contact us and provide details if you believe this document breaches copyrights.
We will remove access to the work immediately and investigate your claim.

PAPER • OPEN ACCESS

Nanofabricated tips for device-based scanning tunneling microscopy

To cite this article: Maarten Leeuwenhoek *et al* 2019 *Nanotechnology* **30** 335702

View the [article online](#) for updates and enhancements.



IOP | ebooksTM

Bringing you innovative digital publishing with leading voices to create your essential collection of books in STEM research.

Start exploring the collection - download the first chapter of every title for free.

Nanofabricated tips for device-based scanning tunneling microscopy

Maarten Leeuwenhoek^{1,2}, Richard A Norte¹, Koen M Bastiaans²,
Doohee Cho², Irene Battisti², Yaroslav M Blanter¹ ,
Simon Gröblacher^{1,3}  and Milan P Allan^{2,3} 

¹ Kavli Institute of Nanoscience, Delft University of Technology, Lorentzweg 1, 2628CJ Delft, The Netherlands

² Leiden Institute of Physics, Leiden University, Niels Bohrweg 2, 2333CA Leiden, The Netherlands

E-mail: s.groeblicher@tudelft.nl and allan@physics.leidenuniv.nl

Received 13 December 2018, revised 10 April 2019

Accepted for publication 25 April 2019

Published 23 May 2019



CrossMark

Abstract

We report on the fabrication and performance of a new kind of tip for scanning tunneling microscopy. By fully incorporating a metallic tip on a silicon chip using modern micromachining and nanofabrication techniques, we realize so-called smart tips and show the possibility of device-based STM tips. Contrary to conventional etched metal wire tips, these can be integrated into lithographically defined electrical circuits. We describe a new fabrication method to create a defined apex on a silicon chip and experimentally demonstrate the high performance of the smart tips, both in stability and resolution. *In situ* tip preparation methods are possible and we verify that they can resolve the herringbone reconstruction and Friedel oscillations on Au(111) surfaces. We further present an overview of possible applications.

Keywords: scanning tunneling microscopy, nanofabrication, device physics

(Some figures may appear in colour only in the online journal)

Scanning tunneling microscopy (STM) is a leading tool for probing electronic and topographic information at the atomic scale [1]. Since its inception a few decades ago, data quality has dramatically improved by focusing on mechanical stability, tip preparation and lower temperatures [2–4]. New possibilities have emerged and greatly extended the range of STM, including quasiparticle interference studies with density of states mapping [5–9], spin-polarized STM [10, 11], and ultra-low temperature operation [2, 12, 13].

Here, we introduce a platform for bringing device-based functionality to STM, with the aim to utilize decades of progress in device engineering for the field of scanning probe. We replace the conventional electrochemically etched, pointy metal wire with an integrated metal tip on a silicon chip. This

new platform, which we call smart tip, allows in principle to directly add additional capabilities to a STM tip, including novel spin-sensitivity, local heating, local magnetic fields, local gating, high-frequency compatible coplanar waveguides, qubits, and double-tips. However, it is *a priori* unclear whether a nanofabricated tip will function for STM measurements, as several challenges arise: the stability needs to be below the picometer scale, stringent requirements exist on the shape and sharpness of the freestanding tip, and contamination from fabrication residues need to be absent. In this paper, we demonstrate the feasibility of nanofabricated tips and the novel smart tip platform. We first discuss our newly developed fabrication procedure and then experimentally show the functionality of these tips in standard STM measurements.

The challenge in realizing smart tips is to make devices that are fully compatible with conventional STM, yet allow for compatibility with standard nano- and microfabrication processes. Specifically we need: (i) a clear protrusion of the tip relative to the underlying chip, (ii) precise control of the tip shape, and (iii) reliable, reproducible fabrication recipes.

³ Authors to whom any correspondence should be addressed.



Original content from this work may be used under the terms of the [Creative Commons Attribution 3.0 licence](https://creativecommons.org/licenses/by/3.0/). Any further distribution of this work must maintain attribution to the author(s) and the title of the work, journal citation and DOI.

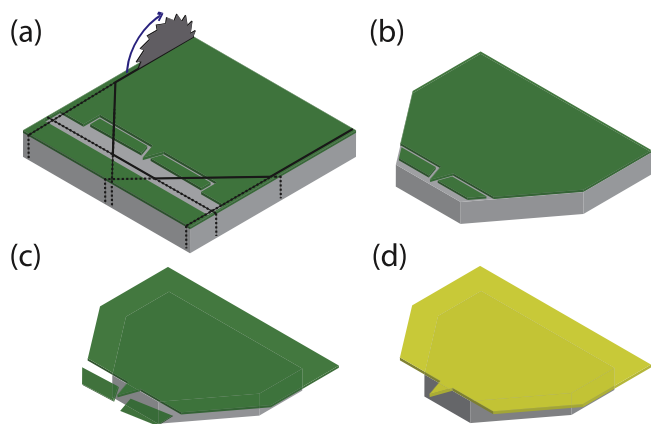


Figure 1. Fabrication procedure for STM smart tips. (a) A layer of SiN (green) covering the Si(100) chip (gray) is patterned through e-beam lithography and plasma etching, creating a large opening and lines that encircle the shields and the tip. (b) The chip is then diced along the black lines. (c) After cleaning, the chip is undercut using a dry release, removing the Si substrate primarily from the sidewalls. The shields are now unsupported and will fall off leaving only the freestanding tip. (d) As a last step, the full chip is covered with a metal, e.g. gold, avoiding residues from the processes before.

To meet these requirements, we developed a new fabrication method using suspended silicon nitride (SiN) tips covered with gold to create on-chip STM smart tips, described below and shown in figure 1.

Using SiN as a base for our suspended STM tips has a number of key advantages. First, it has a large selectivity to the Si etch we use to suspend the tip, allowing for clear protrusions. Making the tips solely out of metal without underlying SiN would also limit the choice of metal to those compatible with the etch described below. Second, it has a high mechanical stiffness, yielding robust tips that are resistant to tip treatment, as discussed later. Finally, it allows for a process where the metallic layer is added as a last step. This allows us to avoid any contamination by chemicals such as etchants and resists.

Our process starts with a $500\ \mu\text{m}$ thick Si(100) chip covered on both sides with a $200\ \text{nm}$ thick layer of high stress low-pressure chemical vapor deposition silicon nitride. We write the initial pattern, consisting of the tip shape and two shields, using electron beam lithography and we then transfer it into the SiN using a reactive-ion CHF_3 etch (see figure 1(a)). The shields are slabs of SiN on both sides of the tip, which we include to minimize the undercut of the Si once the overhang is created: the $50\ \text{nm}$ lines around the shields reduce the etch rate of the Si significantly compared to a large exposed region without shields. We then clean the chip in a piranha solution to remove all traces of resist and protect it in a new layer of photoresist that can be easily removed later by acetone. In order to bring the tip close to the edge we proceed with dicing the chip along the lines depicted in figure 1(a) resulting in figure 1(b). This step is typically precise to within a few micrometers, leaving a straight sidewall (roughness $<3\ \mu\text{m}$). The residue created by the dicing process is washed away with the removal of the protective photoresist layer. After this cleaning step, we isotropically remove part of the Si

substrate using a dry reactive-ion etch (SF_6). For improved selectivity of the SiN over the Si the chip is cooled to $-50\ ^\circ\text{C}$. During a typical etch the thickness of the SiN reduces from 200 to $\sim 120\ \text{nm}$. The exposed Si sidewalls are removed at a rate of around $4\ \mu\text{m}\ \text{min}^{-1}$ until both the tip and the two shields protrude by about $10\text{--}12\ \mu\text{m}$, causing the shields to fall off (figure 1(c)). The straight sides next to the tip can be made very small or even rounded to avoid accidental touches when aligning to a sample, this would not have been possible using an anisotropic KOH wet etch. The final step in fabricating the STM tip involves depositing a metal on the chip through sputtering to ensure proper coverage of both the top and the side of the SiN tip (figure 1(d)). In this study, we choose to deposit $20\ \text{nm}$ of gold using a Leica ACE200 as the tip material; it is relatively straightforward to use other interesting materials for the tip.

Images of a typical device are shown in figures 2(a)–(c). The diameter of the apex of the tip depends on the initial thickness of the SiN, the electron beam spot size and dose, the SF_6 etch time and temperature, and the metal film thickness. However, as can be seen from figure 2(c), the tip diameter is mostly determined by the grain size of the metal film. Our tips achieve radii of a few nanometers, is comparable to specialized commercially available metal wire tips. The overall yield of the fabrication as described in this section is around 80%.

Our microfabricated tips rely on and are compatible with existing STM systems and only requires the modification of the tip holder. In this study, we loaded the tips into a modified commercial Unisoku 1500 ultra-high vacuum STM with an operating temperature down to $2.3\ \text{K}$. We customized the BeCu holder for the smart tips, as shown in figure 2(d). The metal covered top side of the chip is placed against the body of the holder and thereby creates a large metal to metal surface to ensure good electrical contact (few Ohms) and a clamp pushes against the bottom of the chip. The chip is placed under an angle of 10° to avoid contact between the Si sidewall of the chip and the sample. As the metal tip is electrically isolated from the Si by the SiN layer and because Si is highly resistive at low temperatures, tunneling can only originate from the metal tip itself.

Next, we demonstrate the performance of the nanofabricated tips, and show that they are fully compatible with STM. For this, we use a single smart tip made from gold. After having verified that such tips routinely achieve atomic resolution without any tip preparation in ambient conditions on freshly cleaved graphite, we move to atomically flat Au(111) for more reliable tests. We use a Au(111) film on mica at $5.8\ \text{K}$ under UHV conditions. The gold surface is prepared by cycles of Ar ion sputtering ($1\ \text{kV}$ at $5 \times 10^{-5}\ \text{mbar}$) and subsequent annealing at $600\ ^\circ\text{C}$ for $1\ \text{min}$. We use standard tip cleaning procedures, such as voltage pulsing up to $-3\ \text{V}$ and mechanical annealing [14, 15]. The latter procedure consists of repeated and controlled indentation of the tip into the surface up to several conductance quanta and leads to a crystalline, atomically sharp tip apex [15]. All these procedures worked repeatedly with our microfabricated tips.

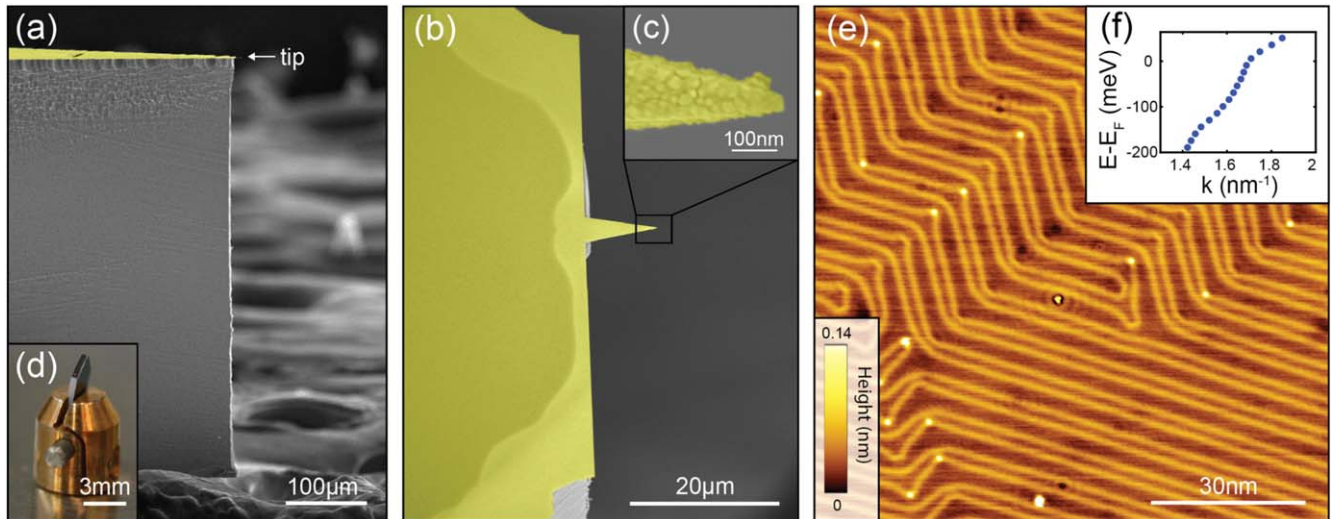


Figure 2. (a)–(c) Scanning electron microscope (SEM) images of a smart tip from the side (a) and the top (b), (c). The freestanding tip made of Au (colored in yellow) covered SiN has a length of $10\ \mu\text{m}$ and a tip radius of approximately $20\ \text{nm}$. The light yellow area is suspended, while the dark yellow parts are still attached to the underlying Si. (c) The tip radius of this particular device is approximately $20\ \text{nm}$. (d) Photograph of a smart tip mounted in our custom BeCu holder. (e) Topograph of Au(111) surface taken with a fabricated tip at $5.8\ \text{K}$ ($V_b = 100\ \text{mV}$, $I = 300\ \text{pA}$). We observe the herringbone surface reconstruction as well as single adatoms (bright dots). In the center a cluster of three adatoms is surrounded by Friedel oscillations. (f) Dispersion of the surface state measured by quasiparticle interference.

Figure 2(e) shows a typical STM image ($99 \times 99\ \text{nm}$) of the reconstructed Au(111) surface obtained with the fabricated tip (setup conditions $100\ \text{mV}$, $300\ \text{pA}$). The herringbone reconstruction characteristic to these gold surfaces is resolved in great detail. Several of the kinks of the reconstruction lines house a single adatom identified as bright spots. Around the three contiguous adatoms in the center of the image, we can observe rings that show the waves of electron scattering, also known as Friedel oscillations. Similarly, quasiparticle interference spectroscopy [7] allows us to measure the dispersion of the surface state, shown in figure 2(f). To quantify the lateral resolution of the tip we extract line traces over the atomic step from the topographic data. The width of the step edge is $1.3\ \text{nm}$, matching with values obtained from measurements with a conventional tip on the same system.

The lateral stability of these tips could be a reason of concern, given their planar nature. Simulations show, however, that the resonance frequency is very high, for both oscillations in the plane and perpendicular to the plane of the tip. Experimentally, we verified that changing the scan direction in the our of plane direction of the tip does not show any difference in the performance of the tip.

We have thus established the functionality of smart tips and that they are fully compatible with existing (commercial) STM systems. We have tested their performance and demonstrated that common tip preparation techniques such as voltage pulses and mechanical annealing can be applied to improve the tip quality *in situ*, which is an important aspect when using STM. For the remainder of this paper, we will discuss applications of these tips.

We would like to highlight some ways of how smart tips can, in the future, contribute to challenges in condensed matter physics and beyond, with an example shown in figure 3. Such applications beyond standard tips are possible

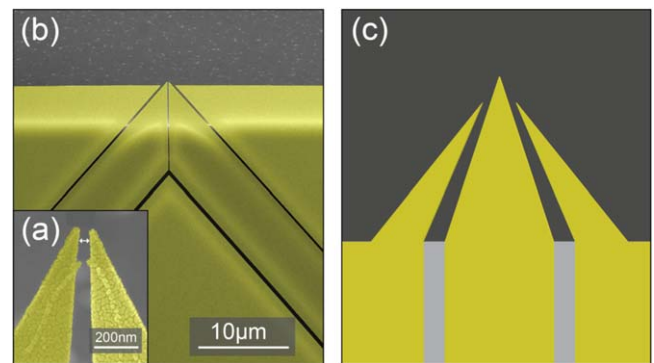


Figure 3. Examples of functionalized smart tips. (a), (b) SEM images of a prototype double-tips to measure the Green's functions. The arrow in (a) indicates a spacing of approx. $45\ \text{nm}$. The two tips (colored in yellow) are electrically completely separated as shown in (b). (c) Conceptual design of a smart tip with a high-frequency compatible coplanar waveguide, which should be easily adaptable from the double-tip design in (b).

as the fabrication recipes allow for a precise control of the tip shape while achieving atomic resolution, which differentiates it from earlier work that relies on cleaving the chip [16–18]. A first example is to guide photons close to the apex of the tip. This can be done for microwave, millimeter and THz waves with coplanar waveguides. There is currently significant research interest in this area [19–23], especially with respect to single spin magnetic resonances, charge dynamics, and (shot) noise measurements on the atomic scale. It is however challenging to control the exact microwave radiation power at the junction and to concentrate the power to the area of interest. This can be solved if the tip itself becomes high-frequency compatible. Our smart tip platform allows to directly include coplanar waveguides on the chip, as depicted

in figure 3(c). This opens a way for improved spin resonance experiments.

A possible application in condensed matter physics is to measure Green's functions, as suggested previously for experiments with two separate tips [24–30]. Such experiments necessitate very short tip-to-tip distances. Recently, much progress has been made with arrangements that rely on multiple conventional tips being brought into close proximity, where the distance between tips are limited by the radii of the tips [31–36], but no Green's function measurement has been possible thus far. Using microfabricated tips has different strengths and weaknesses compared to these approaches. The smart tips can be implemented in compact, ultrastable STM's and are brought into tunneling simultaneously. Micro-fabrication allows to lithographically define both the distance, as well as the shape of the tips. We realize a first proof-of-principle demonstration of this new technique by adapting our single-tip into a two-tip pattern, where the trenches between the tips ensure electrical isolation (see figure 3). This demonstrates that that we can fabricate tip distances smaller than 50 nm. Further work will concentrate on bringing both tips in tunneling simultaneously, e.g. by mounting them on a piezo to allow for a slight tilt. Mechanical annealing [14, 15, 37, 38] can then be used to obtain tips with equal length. The tips then need to be tested on Au(111) samples to ensure that they have the same properties.

Further, one could fabricate a gate that is only nanometers away from the probing tip, using a geometry similar to the one shown in figure 3(b) [18]. Bringing this to the atomic scale allows to image individual donors and their environment in semiconductors and quantum materials. Importantly, there is a large set of quantum materials that are challenging to gate, including high-temperature superconductors. While back- and liquid ion gating had some success [39], material issues prevent large tuning or to differentiate between field and chemical gating [40, 41]. We think that this could be especially beneficial in materials with poor electronic screening [42].

And lastly, the measurement of transport through single molecules, thus far the domain of break junctions [43], can be accessed with smart tips which consist of two tips in close proximity. This has the advantage that one can control where to 'contact' the molecules, and one can measure molecules that are not accessible with standard techniques.

Most importantly, our fabrication recipes allow for easy integration of any standard cleanroom procedure without impeding the STM performance, and therefore new ideas can readily be integrated.

Acknowledgments


We acknowledge valuable support from the Kavli Nanolab Delft, in particular from C de Boer and M Zuiddam. This project was financially supported by the European Research Council (ERC StG Strong-Q and SpinMelt) and by the Netherlands Organisation for Scientific Research (NWO/OCW), as

part of the Frontiers of Nanoscience program, as well as through Vidi Grants (680-47-536, 680-47-541/994).

ORCID iDs

Yaroslav M Blanter  <https://orcid.org/0000-0002-7956-9966>

Simon Gröblacher  <https://orcid.org/0000-0003-3932-7820>

Milan P Allan  <https://orcid.org/0000-0002-5437-1945>

References

- [1] Chen C J 1993 *Introduction to Scanning Tunneling Microscopy* (Oxford: Oxford University Press)
- [2] Song Y J, Otte A F, Shvarts V, Zhao Z, Kuk Y, Blankenship S R, Band A, Hess F M and Strosio J A 2010 Invited review article: a 10 mk scanning probe microscopy facility *Rev. Sci. Instrum.* **81** 121101
- [3] Pan S H, Hudson E W and Davis J C 1999 He refrigerator based very low temperature scanning tunneling microscope *Rev. Sci. Instrum.* **70** 1459
- [4] Battisti I, Verdoes G, van Oosten K, Bastiaans K M and Allan M P 2018 Definition of design guidelines, construction and performance of an ultra-stable scanning tunneling microscope for spectroscopic imaging *Rev. Sci. Instrum.* **89** 123705
- [5] Crommie M, Lutz C and Eigler D 1993 Imaging standing waves in a two-dimensional electron gas *Nature* **363** 524–7
- [6] Petersen L, Hofmann P, Plummer E and Besenbacher F 2000 Fourier transform-stm: determining the surface fermi contour *J. Electron Spectrosc. Relat. Phenom.* **109** 97–115
- [7] Fujita K, Hamidian M, Firmo I, Mukhopadhyay S, Kim C K, Eisaki H, Uchida S-I and Davis J C 2015 Spectroscopic imaging STM: atomic-scale visualization of electronic structure and symmetry in underdoped cuprates *Strongly Correlated Systems: Experimental Techniques* ed A Avella and F Mancini (Berlin: Springer) pp 73–109
- [8] Yazdani A, da Silva Neto E and Aynajian P 2016 Spectroscopic imaging of strongly correlated electronic states *Annu. Rev. Condens. Matter Phys.* **7** 11–33
- [9] Fischer Ø, Kugler M, Maggio-Aprile I, Berthod C and Renner C 2007 Scanning tunneling spectroscopy of high-temperature superconductors *Rev. Mod. Phys.* **79** 353
- [10] Wiesendanger R 2009 Spin mapping at the nanoscale and atomic scale *Rev. Mod. Phys.* **81** 1495–550
- [11] Bode M 2003 Spin-polarized scanning tunnelling microscopy *Rep. Prog. Phys.* **66** 523–82
- [12] Assig M, Eitzkorn M, Enders A, Stiepany W, Ast C R and Kern K 2013 A 10 mk scanning tunneling microscope operating in ultra high vacuum and high magnetic fields *Rev. Sci. Instrum.* **84** 033903
- [13] Von Allwörden H, Eich A, Knol E J, Hermenau J, Sonntag A, Gerritsen J W, Wegner D and Khajetoorians A A 2018 Design and performance of an ultra-high vacuum spin-polarized scanning tunneling microscope operating at 30 mK and in a vector magnetic field *Rev. Sci. Instrum.* **89** 1–9
- [14] Castellanos-Gomez A, Rubio-Bollinger G, Garnica M, Barja S, de Parga A L V, Miranda R and Agrait N 2012 Highly reproducible low temperature scanning tunneling microscopy and spectroscopy with *in situ* prepared tips *Ultramicroscopy* **122** 1–5
- [15] Tewari S, Bastiaans K M, Allan M P and van Ruitenbeek J M 2017 Robust procedure for creating and characterizing the

- atomic structure of scanning tunneling microscope tips *Beilstein J. Nanotechnol.* **8** 2389–95
- [16] Flöhr K, Sladek K, Yusuf Günel H, Ion Lepsa M, Hardtdegen H, Liebmann M, Schäpers T and Morgenstern M 2012 Scanning tunneling microscopy with InAs nanowire tips *Appl. Phys. Lett.* **101** 14–7
- [17] Siahaan T, Kurnosikov O, Barcones B, Swagten H J M and Koopmans B 2016 Cleaved thin-film probes for scanning tunneling microscopy *Nanotechnology* **27** 03LT01
- [18] Gurevich L, Canali L and Kouwenhoven L P 2000 Scanning gate spectroscopy on nanoclusters *Appl. Phys. Lett.* **76** 384–6
- [19] Baumann S, Paul W, Choi T, Lutz C P, Ardavan A and Heinrich A J 2015 Electron paramagnetic resonance of individual atoms on a surface *Science* **350** 417–20
- [20] Donati F *et al* 2016 Magnetic remanence in single atoms *Science* **352** 318–21
- [21] Paul W, Yang K, Baumann S, Romming N, Choi T, Lutz C P and Heinrich A J 2017 Control of the millisecond spin lifetime of an electrically probed atom *Nat. Phys.* **13** 403
- [22] Cocker T L, Peller D, Yu P, Repp J and Huber R 2016 Tracking the ultrafast motion of a single molecule by femtosecond orbital imaging *Nature* **539** 263
- [23] Cocker T L, Jelic V, Gupta M, Molesky S J, Burgess J A, De Los Reyes G, Titova L V, Tsui Y Y, Freeman M R and Hegmann F A 2013 An ultrafast terahertz scanning tunnelling microscope *Nat. Photon.* **7** 620
- [24] Niu Q, Chang M C and Shih C K 1995 Double-tip scanning tunneling microscope for surface analysis *Phys. Rev. B* **51** 5502–5
- [25] Byers J M and Flatté M E 1995 Probing spatial correlations with nanoscale two-contact tunneling *Phys. Rev. Lett.* **74** 306
- [26] Settnes M, Power S R, Petersen D H and Jauho A-P 2014 Theoretical analysis of a dual-probe scanning tunneling microscope setup on graphene *Phys. Rev. Lett.* **112** 096801
- [27] Settnes M, Power S R, Petersen D H and Jauho A-P 2014 Dual-probe spectroscopic fingerprints of defects in graphene *Phys. Rev. B* **90** 035440
- [28] Khotkevych N, Kolesnichenko Y and van Ruitenbeek J 2011 Quantum interference effects in a system of two tunnel point-contacts in the presence of single scatterer: simulation of a double-tip stm experiment *Low Temp. Phys.* **37** 53–8
- [29] Gramespacher T and Büttiker M 1998 Quantum shot noise at local tunneling contacts on mesoscopic multiprobe conductors *Phys. Rev. Lett.* **81** 2763–6
- [30] Gramespacher T and Büttiker M 1999 Local densities, distribution functions, and wave-function correlations for spatially resolved shot noise at nanocontacts *Phys. Rev. B* **60** 2375–90
- [31] Boggild P, Hansen T M, Kuhn O, Grey F, Junno T and Montelius L 2000 Scanning nanoscale multiprobes for conductivity measurements *Rev. Sci. Instrum.* **71** 2781–3
- [32] Jaschinsky P, Coenen P, Pirug G and Voigtländer B 2006 Design and performance of a beetle-type double-tip scanning tunneling microscope *Rev. Sci. Instrum.* **77** 093701
- [33] Roychowdhury A, Gubrud M, Dana R, Anderson J, Lobb C, Wellstood F and Dreyer M 2014 A 30 mk, 13.5 t scanning tunneling microscope with two independent tips *Rev. Sci. Instrum.* **85** 043706
- [34] Kolmer M, Olszowski P, Zuzak R, Godlewski S, Joachim C and Szymonski M 2017 Two-probe stm experiments at the atomic level *J. Phys.: Condens. Matter* **29** 444004
- [35] Ge J-F, Liu Z-L, Gao C-L, Qian D, Liu C and Jia J-F 2015 Development of micro-four-point probe in a scanning tunneling microscope for *in situ* electrical transport measurement *Rev. Sci. Instrum.* **86** 053903
- [36] Hasegawa S 2007 Multi-probe scanning tunneling microscopy *Scanning Probe Microscopy: Electrical and Electromechanical Phenomena at the Nanoscale* ed S Kalinin and A Gruverman (New York, NY: Springer) pp 480–505
- [37] Sabater C, Untiedt C, Palacios J and Caturla M J 2012 Mechanical annealing of metallic electrodes at the atomic scale *Phys. Rev. Lett.* **108** 205502
- [38] Rodrigo J, Suderow H, Vieira S, Bascones E and Guinea F 2004 Superconducting nanostructures fabricated with the scanning tunnelling microscope *J. Phys.: Condens. Matter* **16** R1151
- [39] Bollinger A T, Dubuis G, Yoon J, Pavuna D, Misewich J and Božović I 2011 Superconductor-insulator transition in $La_2-x sr_x cuo_4$ at the pair quantum resistance *Nature* **472** 458
- [40] Dubuis G, Yacoby Y, Zhou H, He X, Bollinger A T, Pavuna D, Pindak R and Božović I 2016 Oxygen displacement in cuprates under ionic liquid field-effect gating *Sci. Rep.* **6** 32378
- [41] Perez-Muñoz A M *et al* 2017 In operando evidence of deoxygenation in ionic liquid gating of $YBa_2Cu_3O_{7-x}$ *Proc. Natl. Acad. Sci. USA* **114** 215–20
- [42] Battisti I, Fedoseev V, Bastiaans K M, de la Torre A, Perry R S, Baumberger F and Allan M P 2017 Poor electronic screening in lightly doped mott insulators observed with scanning tunneling microscopy *Phys. Rev. B* **95** 235141
- [43] Nitzan A and Ratner M A 2003 Electron transport in molecular wire junctions *Science* **300** 1384–9